Biophysical Journal Volume 68 May 1995 1966–1979

A Cross-Bridge Model that Is Able to Explain Mechanical and Energetic Properties of Shortening Muscle

Gabriella Piazzesi and Vincenzo Lombardi
Dipartimento di Scienze Fisiologiche, Università degli Studi di Firenze, 50134 Firenze, Italy

ABSTRACT The responses of muscle to steady and stepwise shortening are simulated with a model in which actin-myosin cross-bridges cycle through two pathways distinct for the attachment-detachment kinetics and for the proportion of energy converted into work. Small step releases and steady shortening at low velocity (high load) favor the cycle implying ~5 nm sliding per cross-bridge interaction and ~100/s detachment-reattachment process; large step releases and steady shortening at high velocity (low load) favor the cycle implying ~10 nm sliding per cross-bridge interaction and ~20/s detachment-reattachment process. The model satisfactorily predicts specific mechanical properties of frog skeletal muscle, such as the rate of regeneration of the working stroke as measured by double-step release experiments and the transition to steady state during multiple step releases (staircase shortening). The rate of energy liberation under different mechanical conditions is correctly reproduced by the model. During steady shortening, the relation of energy liberation rate versus shortening speed attains a maximum (~6 times the isometric rate) for shortening velocities lower than half the maximum velocity of shortening and declines for higher velocities. In addition, the model provides a clue for explaining how, in different muscle types, the higher the isometric maintenance heat, the higher the power output during steady shortening.

INTRODUCTION

According to a widely accepted view (A. F. Huxley, 1957), force and shortening in muscle are generated by cyclic interactions of the myosin heads (the cross-bridges), extending from the thick filaments, with specific sites on the thin actin filaments. The force generated in each interaction is due to a 1000/s structural change (the working stroke) in the myosin head (H. E. Huxley, 1969; Huxley and Simmons, 1971), as confirmed by recent combined mechanical and time-resolved structural experiments (Irving et al., 1992). When the muscle is allowed to shorten, the distance of relative sliding between the two sets of filaments in one cross-bridge cycle is estimated to be 11–14 nm from stepwise length perturbation experiments (Huxley and Simmons, 1971; Piazzesi et al., 1992). During steady shortening, a force lower than the isometric value is maintained by cyclic asynchronous cross-bridge interactions (Huxley, 1957) occurring at rates one to two orders of magnitude lower than that of the elementary force-generating step.

The energy for the work done by the cross-bridge during each cycle of attachment, force generation in the direction of shortening and detachment is thought to be provided by the coupled hydrolysis of one molecule of ATP (Lymn and Taylor, 1971; A. F. Huxley, 1974, 1980). In fact, during shortening at moderate speed, the rate of ATP hydrolysis increases with respect to the isometric value (Kushmerick and Davies, 1969) in accordance with the increase of the rate of energy liberation (Fenn, 1924; Hill, 1938). On the other hand, during shortening at speeds higher than one half the unloaded shortening speed, whereas the rate of total energy liberation remains high, the ATPase rate decreases (Homsher et al., 1981) despite the fact that a significant fraction of isometric cross-bridges (30%, Ford et al., 1985) is interacting. In addition, during forcible lengthening the rate of cross-bridge interactions increases with lengthening speed, whereas ATPase rate decreases (Infante et al., 1964). Thus, the coupling between the cross-bridge cycle and ATP splitting could be not as tight as conventionally supposed. Recent experiments (Lombardi et al., 1992; Irving et al., 1992) suggest that more than one working stroke can occur within a single ATPase cycle. When multiple shortening steps of ~ 5 nm are imposed on a fiber, both the mechanical and the structural manifestation of the working stroke are regenerated within 15 ms, a time much shorter than the 100 ms of the ATP-splitting period (Kushmerick and Davies, 1969).

It has been possible to simulate both mechanical and structural responses during stepwise shortening (Irving et al., 1992; Piazzesi et al., 1993) with a kinetic cross-bridge model originally proposed to explain steady state and transient responses of the muscle during forcible lengthening (Lombardi and Piazzesi, 1990; Piazzesi et al., 1992). The model, which incorporated Huxley's (1957) theory and Huxley and Simmons' (1971) theory, implies the possibility of a strain-dependent detachment of cross-bridges at an intermediate stage of the working stroke followed by rapid reattachment (200 times faster than the attachment from the detached state attained at the end of the cycle) further along the actin filament in a configuration mechanically similar to that at the beginning of the working stroke. This model, however, has several drawbacks. 1) For some reactions in the cycle, the rate constants of state transition are not correctly related to the free energy functions of the corresponding states (T. L. Hill, 1974); 2) as a consequence of the first point, it is not

Received for publication 15 April 1994 and in final form 14 October 1994.
Address reprint requests to Dr. Vincenzo Lombardi, Dipartimento di Scienze Fisiologiche, Università degli Studi di Firenze, Viale G. B. Morgagni 63, 50134 Firenze, Italy. Tel.: 39-55-423-7307; Fax: 39-55-437-9506; E-mail: lmbpzz@stat.ds.unifi.it.

0006-3495/95/05/1966/14 $2.00

possible to evaluate the flux of energy accompanying cross-bridge cycling through the different pathways; 3) the fraction of myosin heads attached to actin in isometric conditions is very high (95%) and cannot be chosen as a free parameter.

Here we present a thermodynamically correct version of the model in which periodic boundary conditions for attachment of a myosin cross-bridge to actin are chosen so that in isometric conditions 77% of myosin heads are attached. The model assumes that cross-bridges cycle through two different pathways, characterized by different kinetics of detachment and reattachment and different efficiency in free energy conversion. The fraction of cross-bridges involved in each pathway depends on the mechanical conditions under which the contraction occurs. Small step releases and steady shortening at low velocity (high load) favor the cycle implying ~5 nm sliding per cross-bridge interaction and ~100/s detachment-reattachment process (short stroke cycle); large step releases and steady shortening at high velocity (low load) favor the cycle implying ~10 nm sliding per cross-bridge interaction and ~20/s detachment-reattachment process (long stroke cycle). The latter cycle is responsible for the working distance measured by the intercept of T_2 curve according to Huxley and Simmons' experiments (1971). The model is able to explain the known mechanical and energetic properties of the contracting muscle, the rate of energy production in isometric conditions and its increase during steady shortening, the dependence of power and efficiency on shortening speed (Hill, 1938, 1939, 1964a, b; Kushmerick and Davies, 1969), and the relation, present among different muscle types, between heat rate in isometric conditions and maximum power output during steady shortening (Woledge et al., 1985; Barclay et al., 1994); moreover, it accounts for the new data in this paper referring to the tension response to multiple step releases (staircase shortening).

The assumption in our model of two pathways of cross-bridge cycling, distinct for kinetics and efficiency in energy conversion, overcomes a common drawback of all models in which cross-bridges cycle through only one pathway and ATP hydrolysis is tightly related to the completion of the working stroke, i.e., the continuous increase in the rate of energy liberation with shortening velocity (Huxley, 1957, 1980; Julian et al., 1974; Eisenberg et al., 1980; Pate and Cooke, 1989).

The description of the properties of the model is divided in three sections: the first section deals with the working stroke and its regeneration, the second section deals with the mechanical and energetic properties during steady shortening, and the third section deals with tension responses to staircase shortening. In each section, the properties of the model are compared with the corresponding experimental data collected as described in Materials and Methods. The experiments reported in the first and second sections have already been described in the literature (Hill, 1938; Huxley and Simmons, 1971; Ford et al., 1977, 1985; Lombardi et al., 1992), and those reported in the third section have been made in collaboration with Marco Linari and have not yet been published in extenso.

MATERIALS AND METHODS

Experimental data

Data were collected from experiments made at 4–5°C and at the resting sarcomere length of about 2.1 μm on single intact fibers dissected from the tibialis anterior muscle of the frog (Rana esculenta). The fiber length ranged from 4.7 to 5.8 mm; the fiber cross sectional area ranged from 6,500 to 10,900 μm^2. The fibers were mounted in the experimental trough between a loudspeaker motor (Cecchi et al., 1976; Lombardi and Piazzesi, 1990) and a capacitance force transducer with natural frequency 50 kHz (Huxley and Lombardi, 1980). The fibers were stimulated with pulse trains of current of 1.5 times the threshold intensity and at a frequency adequate to produce fused tetani of 0.5–1 s duration. The actual change in length of a segment (0.9–1.9 mm long) selected along the fiber near the force transducer end was controlled by a striation follower (Huxley et al., 1981). The fiber response started in fixed-end mode (the servo system for length control uses as feed-back signal the position of the motor lever), and the control was shifted to segment length-clamp mode (the feed-back signal is the segment length) at the end of the rising phase of the isometric tetanus. To elicit tension transients, single or double steps in sarcomere length (1–11 nm per half-sarcomere (h.s.) amplitude, complete within 120 μs) were applied at a preset time during the tetanus plateau. Tension responses to steady and staircase shortening were determined by imposing ramp or multiple-step shortening for a total amount of filament sliding not larger than 50 nm per h.s., so as to maintain the sarcomere length in the plateau region of the tension-sarcomere length relation (Gordon et al., 1966). The control was shifted back to the fixed-end mode during tetanic relaxation. The stiffness of the fiber, which under the experimental conditions used gives an estimate of the number of attached cross-bridges, was determined either at the plateau of the isometric tetanus or during the steady force response to shortening by superposing steps in sarcomere length of amplitude ~1.5 nm per h.s.

Model computation

The simulation is based on the cross-bridge model already described to simulate steady-state and transient responses during forcible lengthening of the tetanized muscle fiber (Lombardi and Piazzesi, 1990; Piazzesi et al. 1992). Discussed here are the modifications introduced to make the model thermodynamically correct and to provide periodic boundary conditions for attachment of myosin to actin. The scheme of cross-bridge reactions is given in Fig. 1 *A*.

D1 and D2 are detached states, and A1, A2, and A3 are attached states. The elementary force-generating step underlying the working stroke is represented by each of the transitions A1 → A2 and A2 → A3: each transition is accompanied by a structural change in the myosin head, the S1 portion, responsible for an extension z = 4.5 nm of the elastic component acting in series with the cross-bridge in the half-sarcomere. The progression of numbers identifying the transitions in each of the two cycles is according to the direction of the reaction flow during steady shortening, as indicated by the circular arrows: steps 1, 2, 3, and 4 identify cycle *l*, in which detachment follows the completion of the working stroke (long stroke cycle); steps 2, 5, and 6 identify cycle *s*, in which detachment occurs at an intermediate stage and is followed by rapid reattachment (short stroke cycle).

A myosin cross-bridge, which repeats along the filament axis with a periodicity of 14.3 nm, can attach only to one actin site for a range of positions λ = 5.5 nm, from x = −1.6 to 3.9 nm (where x is the relative axial position between the myosin head and the actin site, taken as zero when the cross-bridge in A1 state exerts zero force). Even if the separation between actin sites is also λ, for simplicity we assumed that in isometric conditions there is no overlap in the interaction of a myosin head with the successive binding sites on the actin filament. The distribution of myosin heads with respect to the actin sites available in the surrounding thin filaments is sparse enough to ensure that there is no interference between the myosin heads for the same actin. Let's call ξ the value x assumes within λ ($-1.6 < \xi < 3.9$). Myosin heads are uniformly distributed along x so that, in isometric conditions, for each value of ξ the sum $N(\xi)$ of all attached $(a_1(\xi),a_2(\xi),a_3(\xi))$, and detached $(d_1(\xi),d_2(\xi))$ cross-bridges is 1.

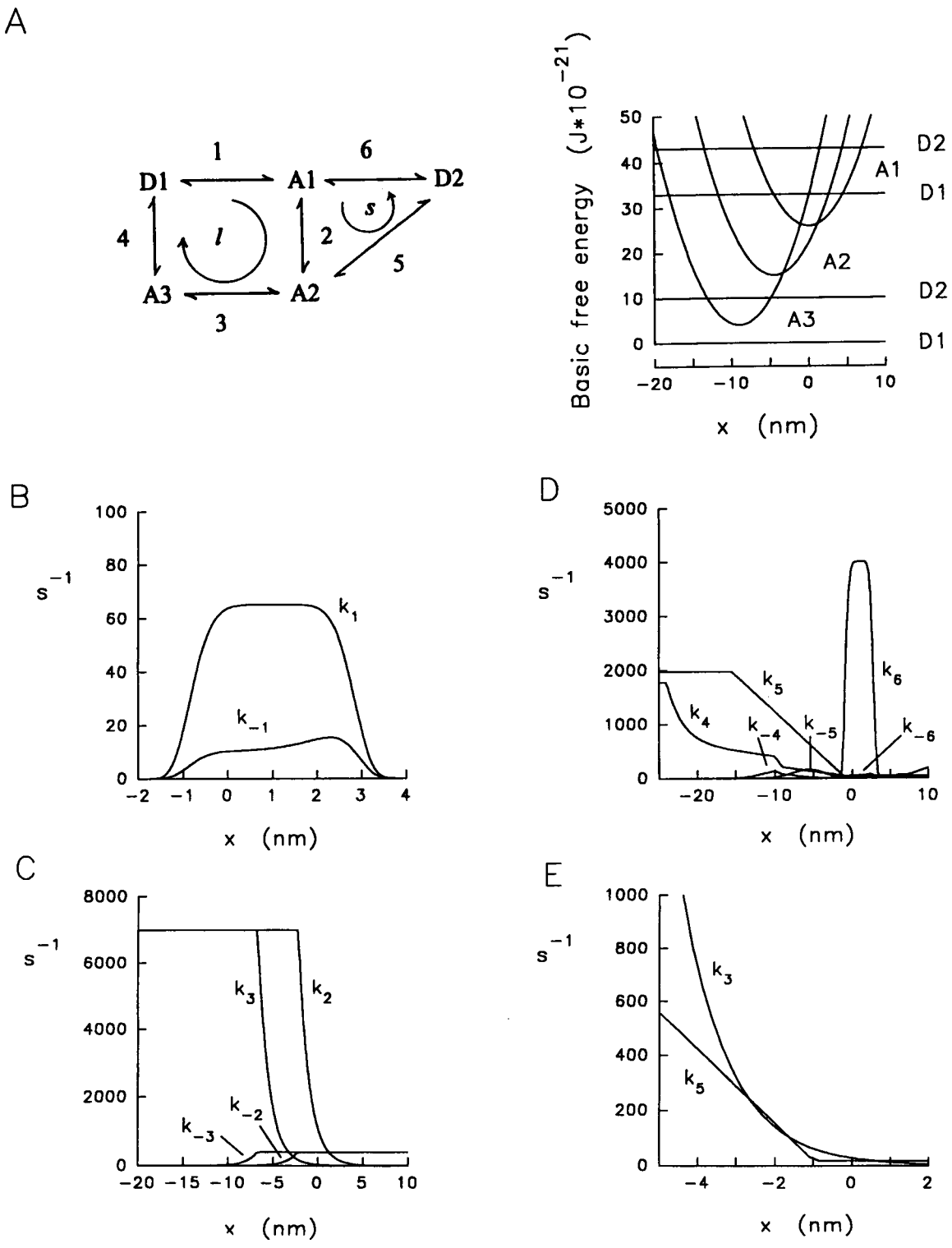

FIGURE 1 (*A*) Scheme of cross-bridge reactions and free energy diagrams of the cross-bridge states as a function of the relative position (x) between the myosin head and an actin site. x is set to zero in correspondence of the minimum free energy of a cross-bridge attached in state A1. During shortening actin binding sites enter from the right. Horizontal lines give the free energy of the detached states. The free energy of state D1 at the end of the cycle is arbitrarily set to zero, and the free energy of all the other states are given relative to this value. (*B–D*) Functions expressing the dependence of the rate constants on x. (*E*) Comparison between k_3 (A2 → A3) and k_5 (A2 → D2) in the region where the two rate constants have similar values.

The periodic boundary conditions imply that at the two extremities of λ in isometric conditions there are practically no attached cross-bridges and d_1 and d_2 have identical values, respectively. Thus, there is continuity in the distribution of each cross-bridge state at the two extremities. Sliding in either shortening (negative x) or lengthening (positive x) direction brings attached cross-bridges to positions beyond the values (−1.6 and 3.9) that limit the

isometric distribution. When a cross-bridge detaches the time for the head to regain the original configuration and for the elastic component to recoil is assumed to be very short (~10 μs) according to the low viscosity of the surrounding medium. Provided that the rate of reverse reaction at the site of detachment is low with respect to the resetting time of the cross-bridge, all of the heads detaching at a given x beyond λ regain the position, within λ, given by $\xi = x - n\lambda$, where n, negative for shortening and positive for lengthening, is the number of times the attached cross-bridge has exceeded one boundary in the same direction. Under these conditions, a myosin head can attach to only one actin site, also during sliding, and there is no contradiction in thermodynamic reversibility at the site of detachment (further consideration of this point is presented in Discussion). During sliding, $N(\xi) = 1$ is given by the equation:

$$N(\xi) = d_1(\xi) + d_2(\xi) + \sum[a_1(\xi + n\lambda) + a_2(\xi + n\lambda) + a_3(\xi + n\lambda)] = 1. \quad (1)$$

The free energy profiles ($G(x)$, Fig. 1 *A*, *right*) of the various states are related to the forward $k_i(x)$ and reverse $k_{-i}(x)$ rate constants of the transition i (=1 ,..., 6) between two neighboring states j and m through the Gibbs equation:

$$k_i(x)/k_{-i}(x) = \exp[(G_j(x) - G_m(x))/k_B\theta], \quad (2)$$

where k_B is the Boltzmann constant and θ is the absolute temperature. In general, the free energy profiles are chosen as a first option to fit mechanical and energetic properties and one rate constant of the pair is calculated from Eq. 2 after choosing the appropriate value for the other.

The assumption that the elasticity acting in series with the active component of the cross-bridge is linear (Huxley and Simmons, 1971; T. L. Hill, 1974) is retained in our model. Therefore, the free energy curves of the attached states have a parabolic profile. According to the considerations made in the previous version of the model (Lombardi and Piazzesi, 1990; Piazzesi et al., 1992), to fit the time course of the quick component of the tension recovery after a step-length perturbation with a three attached state model, limits must be set to the drop in free energy between two consecutive attached states and, consequently, to the steepness of the parabolas representing the free energy profiles of the attached states. As in the previous version, the difference in free energy minima for either transition A1 → A2 and A2 → A3 is $11 \cdot 10^{-21}$ J or 11 pnJ, and the value of the second derivative of the parabolas, the stiffness of the series elastic component, is 0.7 pN/nm. The average extension of the elastic component at the plateau of the isometric tetanus must be ~3.6 nm, according to the experimental results (Ford et al., 1977, 1981; Piazzesi et al., 1992). Thus, the isometric force per attached cross-bridge is (0.7 pN/nm · 3.6 nm=) 2.5 pN. This value implies a high value for the fraction of myosin heads involved in force generation at the steady state in isometric conditions. In fact, in a frog muscle fiber developing an isometric tetanic tension (T_0) of 290 kN/m^2, with 500 myofilaments/μm^2 and 300 heads/hemifilament, the force per myosin head (F_0) is 1.9 pN and 77% of the myosin heads must contribute to force, to have a force per attached head of 2.5 pN. Actually, stiffness measurements and structural data suggest that a large fraction of myosin heads are attached in isometric conditions (Matsubara et al., 1975; Goldman and Simmons, 1977; H. E. Huxley et al., 1980).

The free energy converted into work for a cross-bridge involved in the long stroke cycle must be ~20 pnJ according to the mechanical energy under the T_2 curve. Thus, to have a maximum efficiency of ~60%, the free energy change through either cycle is assumed to be 33 pnJ.

For any steady-state mechanical condition (at the isometric plateau or during steady shortening), the total flux of energy ($\dot{E}$) can be calculated from the fluxes of cross-bridges through both cycles. Assuming that the free energy of the hydrolysis of ATP (ΔG_{ATP}) in the physiological condition is 100 pnJ (Bagshaw, 1993), it follows that on average cross-bridges can detach and reattach with energy consumption (100 pnJ/33 pnJ=) 3 times/molecule of ATP hydrolyzed.

The diagram of the free energy functions for the various states is shown in Fig. 1 *A*. The states are defined only for their mechanical and kinetic properties, ignoring the underlying biochemical state. The free energy level of a cross-bridge in either state A1 or A2 for a given value of x has a unique value independent of the pathway through which the state has been populated. D1 differs from D2 not only kinetically but also for the amount of the difference in free energy with respect to the nearest attached state.

The equations expressing the x dependence of the reaction rates are given in Table 1 and the corresponding plots are shown in Fig. 1 *B–E*.

The form of differential equations to calculate the rates of the transitions between consecutive states is given by A. F. Huxley's 1957 paper and for the present model the equations are the following:

$$\frac{\delta a_1(x,t)}{\delta t} = k_1(x)d_1(x,t) + k_{-2}(x)a_2(x,t) + k_6(x)d_2(x,t) - (k_{-1}(x) + k_2(x) + k_{-6}(x))a_1(x,t) - \nu\frac{\delta a_1(x,t)}{\delta x}$$

$$\frac{\delta a_2(x,t)}{\delta t} = k_2(x)a_1(x,t) + k_{-3}(x)a_3(x,t) + k_{-5}(x)d_2(x,t) - (k_{-2}(x) + k_3(x) + k_5(x))a_2(x,t) - \nu\frac{\delta a_2(x,t)}{\delta x}$$

$$\frac{\delta a_3(x,t)}{\delta t} = k_3(x)a_2(x,t) + k_{-4}(x)d_1(x,t) - (k_{-3}(x) + k_4(x))a_3(x,t) - \nu\frac{\delta a_3(x,t)}{\delta x} \quad (3)$$

$$\frac{\delta d_1(x,t)}{\delta t} = k_{-1}(x)a_1(x,t) + k_4(x)a_3(x,t) - (k_1(x) + k_{-4}(x))d_1(x,t) - \nu\frac{\delta d_1(x,t)}{\delta x}$$

$$\frac{\delta d_2(x,t)}{\delta t} = k_{-6}(x)a_1(x,t) + k_5(x)a_2(x,t) - (k_6(x) + k_{-5}(x))d_2(x,t) - \nu\frac{\delta d_2(x,t)}{\delta x},$$

where ν is the velocity of sliding between filaments.

The cross-bridge distribution at any given time was calculated by numerical integration of the differential equations by means of Euler method. In isometric conditions, the time step for integration was 100 μs. The simulation started with all cross-bridges in the D1 state. Fractions of cross-bridges in each state were calculated at x-points separated by an interval (Δx)

TABLE 1 Equations expressing x-dependence of the rate constants of the forward transitions according to the direction of the reaction flow during steady shortening, as defined in the text

$k_1(s^{-1})$	$= 65 \cdot \exp(-0.02(x-1)^6)$	
$k_2(s^{-1})$	$= 7000$	$x < -\frac{z}{2}$
	$= 7000 \cdot \exp(-\frac{1}{2}\epsilon(2xz + z^2)/k_B\theta)$	$x \geq -\frac{z}{2}$
$k_3(s^{-1})$	$= 7000$	$x < -\frac{3}{2}z$
	$= 7000 \cdot \exp(-\frac{1}{2}\epsilon(2(x+z)z + z^2)/k_B\theta)$	$x \geq -\frac{3}{2}z$
$k_4(s^{-1})$	$= 1776$	$x < -24$
	$= 399 + \exp(-0.5(x+10)) - 20(x+10)$	$-24 \leq x < -10$
	$= -200(x+8)$	$-10 \leq x < -9$
	$= -20(x-1)$	$-9 \leq x < -1$
	$= 40$	$x \geq -1$
$k_5(s^{-1})$	$= 1975$	$x < -15.5$
	$= -135(x+0.867)$	$-15.5 \leq x < -1$
	$= 18$	$x \geq -1$
$k_6(s^{-1})$	$= 4000 \cdot \exp(-0.02(x-1)^6)$	

ϵ, the stiffness of the elasticity acting in series with the cross-bridges, is 0.7 pN nm^{-1}; k_B, the Boltzmann constant, is $1.3805 \cdot 10^{-2}$ pN nm K^{-1}; θ, the absolute temperature, is 277.16 K.

of 0.05 nm from each other. The values of the ks were considered constant within this interval. Because D1 cross-bridges exist only within λ ($-1.6 < x < 3.9$), there are (5.5/0.05=) 110 discrete positions for which the isometric distribution is calculated. The fractional occupancy of the various states at the steady state of the isometric contraction is shown as function of x in Fig. 2. The proportion of cross-bridges in each state, averaged among the 110 positions, is listed near the graph. Attached cross-bridges are in total 77% of all available cross-bridges.

During isovelocity shortening, the time step for numerical integration was chosen according to the sliding velocity: for velocities lower than 0.7 μm/s, it was set to 40 μs, for higher velocities it was determined by the ratio of Δx over the velocity.

For simulating the transient after a step length change, the time step was 20 μs. In each particular condition, time steps shorter than those selected gave the same results. For the sake of simplicity, the step-length change was considered to be complete in zero time. Consequently, the simulated relation of tension attained at the end of the length step versus the amplitude of the length step is not affected by the quick tension recovery which, in the experimental relation, produces a deviation from linearity (Ford et al., 1977). It is evident from the comparison in Fig. 3 that, with the step releases used in the experiments reported here (complete within 120 μs), the difference becomes significant only in the region of large step releases.

The stiffness of the elastic component in series with the active component of the cross-bridge (ϵ) was assumed to be constant independent of cross-bridge state or strain. Under these conditions, the stiffness (S) in a given simulated response was measured by the number of attached cross-bridges.

The force generated by an attached cross-bridge (F_x) between $x - \Delta x/2$ and $x + \Delta x/2$ was given by $\epsilon[xa_{1,x} + (x + z)a_{2,x} + (x + 2z)a_{3,x}]$. The total force generated by the population of the attached cross-bridges (called T, in analogy with the force measured in the experiments) was calculated by integrating F_x over x. When tension responses from experiment and model are superposed, the simulated tension is multiplied by the ratio of T_0 for the experiment over T_0 for the model (290 kN/m^2, with a force per myosin head, F_0, 1.93 pN) to make the comparison independent of the variability of T_0 between different fibers.

RESULTS

The working stroke and its regeneration

According to the work by Huxley and co-workers (Huxley and Simmons, 1971; Ford et al., 1977, 1981), the tension transient after a step perturbation in sarcomere length represents specific events in the cross-bridge cycle of activity. As shown in Fig. 3 *A*, after the elastic response simultaneous with the step (phase 1 of the transient) there is a quick recovery (phase 2) complete within the first few milliseconds, which is attributed to the synchronous execution by cross-bridges of the elementary force-generating step, the working stroke. Evidence for the complex nature of this viscous-like response is given by the finding that the rate of quick tension recovery increases going from the stretch to the largest release.

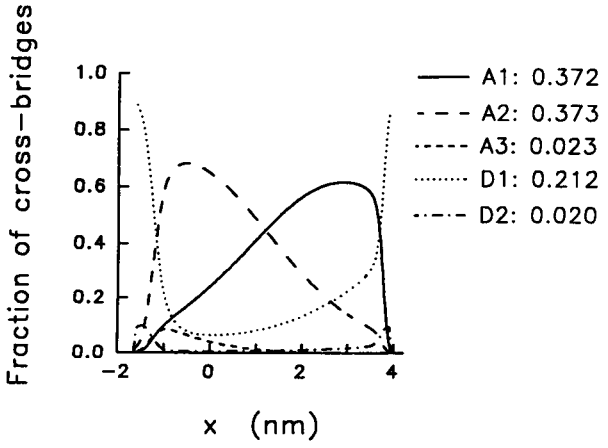

FIGURE 2 Fraction of cross-bridges in the various states as a function of x at the steady state of an isometric contraction. Figures in the inset indicate the number of cross-bridges in each state relative to the total number of heads.

The simulated quick recovery elicited by length steps of different size is compared with the experimental one in Fig. 3 *A*. For the releases, the characteristics of the experimental records are satisfactorily reproduced by the model. For the stretch, the simulated response fails to fit the experimental one in two aspects: 1) the very early component is too slow; 2) starting 4–5 ms after the step, the two traces diverge because in the simulated one there is not a late component of the quick recovery. These failures have been already shown in a previous paper (Piazzesi et al., 1992, Fig. 26) and could be related to processes other than the redistribution between different force-generating states of the attached cross-bridges.

Fig. 3 *B* shows the plots of T_1, the extreme tension attained during the step, and T_2, the value of tension recovered at the end of phase 2 (estimated by the tangent method, Ford et al. 1977), versus step amplitude.

In general, the simulated T_1 and T_2 curves superimpose satisfactorily on the experimental ones, with the exception of T_2 points for stretches, which lie above, because of the absence of the late component of quick recovery. This explains also why the relation of r (the rate constant of quick tension recovery, estimated by the time necessary to attain 63% of T_2) versus step amplitude deviates upward in the region of stretches with respect to the experimental one (Fig. 3 *C*).

As already discussed in a previous paper (Piazzesi et al., 1992), phase 2 of the tension transient is simulated by incorporating in our model Huxley and Simmons' theory for force generation: the tension recovery within the first 2 ms after a length step is mainly related to redistribution between different force-generating states of the attached cross-bridges. A key assumption in Huxley and Simmons' model is that the mechanical energy in the attached cross-bridge is part of the activation energy for the state transition in the force-generating process: the larger the shift of the cross-bridge distribution toward negative x, the higher the value of the rate constants k_2 and k_3 and, consequently, the rate of quick recovery (Fig. 3 *C*).

As shown by Fig. 3 *D*, phase 2 of the recovery is followed by a pause or even a reversal of the tension recovery (phase 3), which is briefer for larger releases. Eventually, the tension approaches the value before the step within about 100 ms (phase 4). Phases 3 and 4 are related to detachment and reattachment further along the actin filament (Huxley and Simmons, 1973; Lombardi et al., 1992).

The process underlying phase 3 after a step release has been clarified by imposing a test step release at different

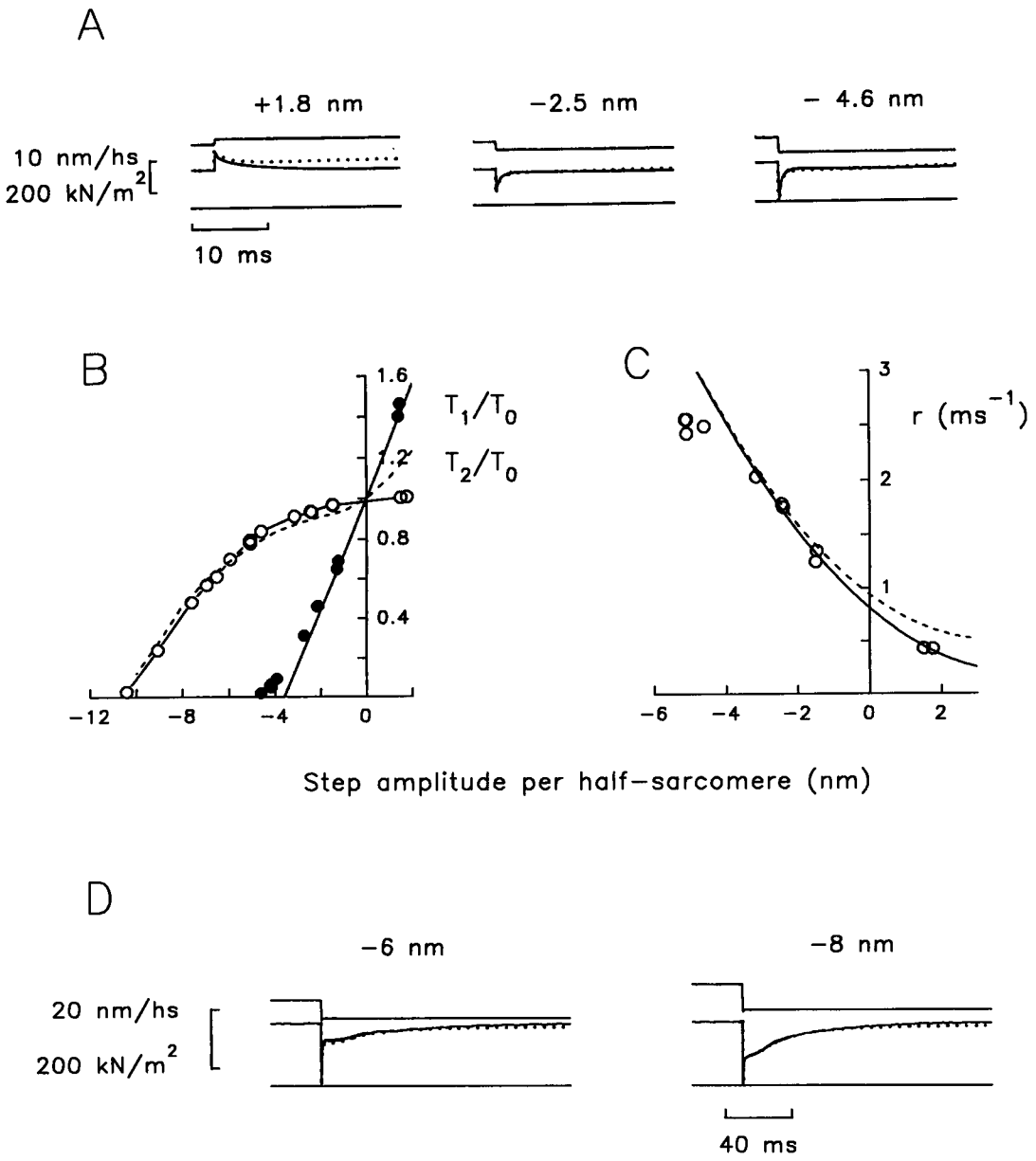

FIGURE 3 (*A*) Early components of tension transients elicited by steps of different size imposed at the steady state of the isometric contraction. In each frame, the upper trace is the sarcomere length change from the experiment, the middle trace is the tension response (——, experiment; · · · · ·, model simulation), and the lower trace is tension baseline. The size of the step in the half-sarcomere is indicated by the figure above the length trace. (*B*) T_1 (● and ——, experiment; - - - -, model) and T_2 (○ and ——, experiment; - - - -, model) curves obtained from responses as in *A* with the same procedure for experiment and simulation. T_1 and T_2 are relative to the tetanic plateau tension (T_0). The straight line interpolated through experimental T_1 points for small steps superposes on the simulated T_1 relation. The abscissa intercept (Y_0) is 3.6 nm. The length axis intercept of experimental T_2 curve is 10.5 nm and coincides with the intercept of the simulated T_2 curve. (*C*) rate of quick tension recovery (r) versus step amplitude (○ and ——, experiment; - - - -, model). r is estimated by the reciprocal of time necessary to attain 63% of the T_2 recovery. The lines are obtained by fitting the r data points with a parabola. The fit for the experiment is done with points obtained for step releases smaller than 4 nm. The points for step releases larger than 4 nm lie below the extrapolated parabola because of the underestimate produced by the truncation of the early component of the tension recovery, when the fiber becomes slack. (*D*) Whole tension transients at low trace speed for step releases larger than in *A*, to emphasize the contribution of phase 4 to the recovery of the original isometric tension. (*top*) Sarcomere length change from the experiment; (*middle*) superposed tension responses (——, experiment; · · · · ·, model); (*bottom*) tension baseline.

times after a conditioning release (Lombardi et al., 1992; Piazzesi et al., 1993). It was shown that within 15 ms after a step release most of the cross-bridges already involved in the partial working stroke elicited by the release have undergone a process of detachment and rapid reattachment further along the actin filament, so that by this time the full working stroke capability was reprimed. Detachment is the rate limiting step in this process, because stiffness remains high during the whole recovery period (90% of the original isometric value with a conditioning step of 5 nm).

The time course of the regeneration of the working stroke can be obtained by plotting, versus the time t elapsed after

the conditioning step, either the intercept of the test T_2 curve (Lombardi et al., 1992) or the proportion of tension recovered at the end of phase 2 after the test step, $(T_2 - T_1)/(T_i - T_1)$, where T_i is the tension attained just before the test step. The latter procedure is much easier (only one size of the test step is necessary) and has been followed here (Fig. 4). Typically, with a 5-nm conditioning step the time constant of the regeneration process is 5–6 ms.

The process of regeneration of the working stroke, made explicit with double step experiments, is due to rapid detachment and reattachment further along the actin filament in the original configuration through steps 5 and 6 in the reaction scheme. In agreement with the experiment (Lombardi et al., 1992), the number of attached cross-bridges remains high during this process (90% of isometric value at 2 ms and 84% at 20 ms), because the rate-limiting step in the process is detachment.

The cycling of cross-bridges through the short or long stroke pathway depends strongly on the amplitude of the step release. During the first few milliseconds after the completion of the quick recovery of force after a 5 nm release, the flux of cross-bridges is predominantly through the short stroke cycle, that is, the process of fast repriming is dominating, because most of cross-bridges are in the region where k_5 and k_3 are comparable. Increasing the size of the step, the flux through the short stroke cycle becomes less and less and the flux through the long stroke cycle increases because cross-bridges move in the region where $k_3 \gg k_5$. Because reattachment in cycle l is a rate-limiting step, the number of attached cross-bridges decreases. In the double-step experiment, a test release of 5 nm applied soon after a conditioning step of 5 nm interrupts the rapid regeneration process, shifting the distribution of attached cross-bridges toward x values that favor long stroke pathway and detachment to D1. If the test release is applied 15 ms later, most of the cross-bridges have regained the isometric distribution and the test release produces the same shift in the x distribution of the attached cross-bridges as a single-step release of the same amplitude. Consequently, just as for a single release of 5 nm, the dominant fluxes are through the short stroke pathway.

Force and energy liberation during steady shortening at different velocities

When a muscle fiber is allowed to shorten at constant velocity, tension drops in a characteristic way dependent on phase 2 of the tension transient (Ford et al., 1977) and then, beyond 12 nm of shortening, approaches a steady value characteristic of Hill's hyperbolic equation (1938).

Steady-state relations of force and stiffness versus velocity of shortening are shown in Fig. 5 *A*. The solid line shows the experimental relation between steady force and velocity of sarcomere shortening (T-V relation) obtained by fitting Hill's hyperbola to mean T-V points (*open symbols*) from nine experiments at 4–5°C. The long dashed line shows the T-V curve fitted to the simulated points. For both curves, data points referring to the region of forces larger than 0.8 T_0 were not used for the fitting procedure because of the deviation of these points from the hyperbolic relation (Edman et al., 1976). The intercept of the curve on the force axis (T_0^*) is 1.29 times (experiment) and 1.38 times (model) the isometric plateau value. The curvature of the relation, expressed by Hill's parameter a/T_0 (0.32, experiment; 0.26, model), as well as the intercept on the velocity axis, V_0 (2.88 μm/s, experiment; 2.67 μm/s, model), which represents the maximum velocity of shortening or the velocity under zero load, are typically within the range of values reported for twitch fibers from frog skeletal muscle at low temperature (Hill, 1938; Katz, 1939; Cecchi et al., 1978; Lännergren, 1978).

The dependence of steady stiffness on velocity of shortening is shown in Fig. 5 *A* by filled symbols (experiment) and the short dashed line (model). It can be seen that the decrease in stiffness with the increase in shortening velocity is less than in proportion with the decrease in force. Thus, the ten-

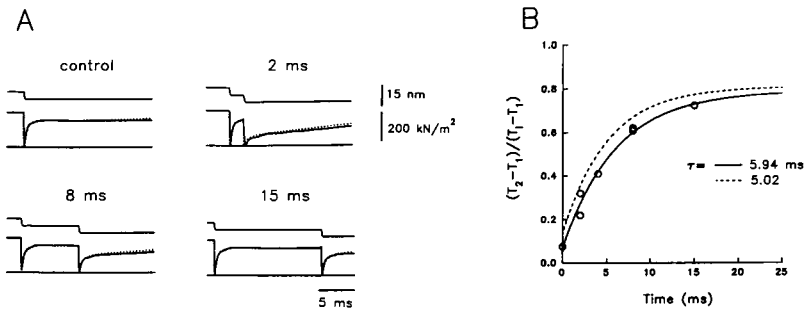

FIGURE 4 (*A*) Tension responses to a length step of 5 nm imposed either at the isometric tetanus plateau (control) or 2, 8, and 15 ms after the conditioning release of 5 nm. In each frame, the upper trace is segment length change from the experiment, the middle trace is tension (——, experiment; · · · · ·, model), and the lower trace is resting tension. (*B*) Circles and solid line: plot of the proportion of tension recovered at the end of phase 2, $(T_2 - T_1)/(T_i - T_1)$, for a test step release of 5 nm versus the time elapsed after the conditioning release of 5 nm in the same fibre as in *A*. The point at zero time is the value of $(T_2 - T_1)/(T_i - T_1)$ for a single step release of 10 nm. The solid line is fitted to the data according to the exponential equation: $m - (m - n)\exp(-t/\tau)$ where m (the estimated value of the ordinate for a single step of 5 nm) = 0.79, n (the estimated value of the ordinate for a single step of 10 nm) = 0.067 and τ (the time constant) = 5.9 ms. (- - - -) Exponential fitted to the simulated points obtained with the same procedure as for experimental points (m = 0.81, n = 0.135, τ = 5.0 ms).

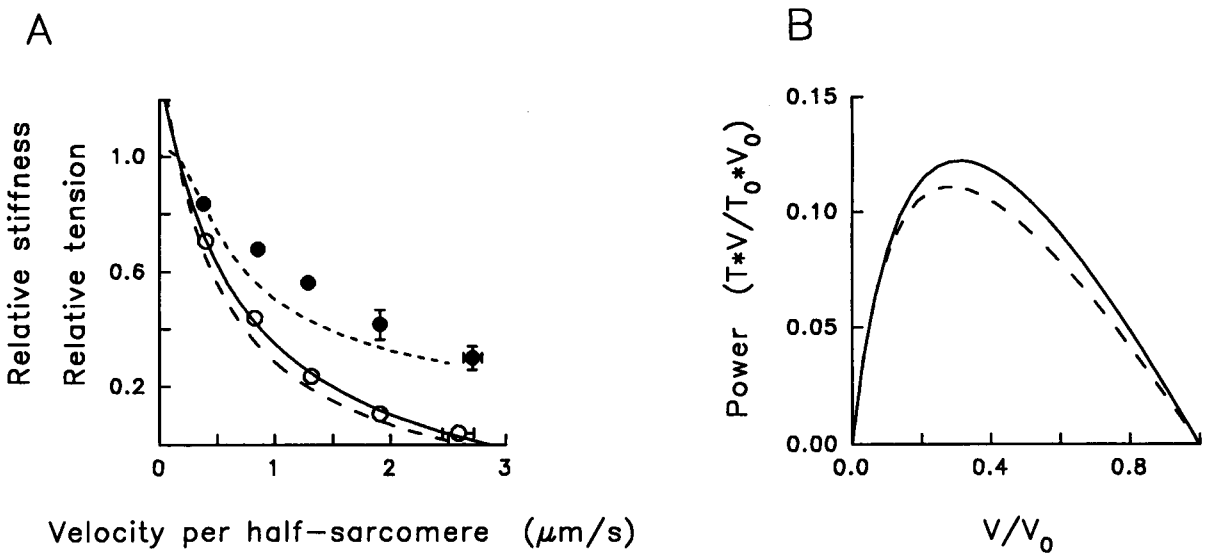

FIGURE 5 (*A*) Experimental relations of tension (○ and ——) and stiffness (●) versus velocity of shortening. Stiffness was measured by small step stretches (1.3 nm) superposed on either the isometric tetanus plateau or the shortening ramp. Tension and stiffness are relative to the isometric plateau value. The points are the means of data obtained from nine fibers (tension) and from five of the nine (stiffness). Data were grouped in classes of velocities ~0.5 μm/s wide. Bars indicate the SEMs; when bars are not visible, it is because their size is smaller than symbol size. The continuous line is Hill's hyperbolic equation fitted to tension points. Hill's parameters are: $a/T_0 = 0.32$, $V_0 = 2.88$ μm/s, $T_0^*/T_0 = 1.29$. Temperature in the nine fibers was 4.71 ± 0.19°C (mean ± SEM). The long dashed line is the force-velocity curve obtained from simulated data. Hill's parameters are: $a/T_0 = 0.26$, $V_0 = 2.67$ μm/s, $T_0^*/T_0 = 1.38$. The short dashed line is the simulated stiffness-velocity relation estimated by the fraction of cross-bridges attached at any velocity with respect to those attached in isometric conditions. (*B*) Power-velocity relations obtained from experimental Hill's equation (——) and from simulated Hill's equation (- - - -). Power and velocity are normalized for V_0.

sion to stiffness ratio (R), a measure of the average force exerted by each cross-bridge, reduces progressively: at 1/3 V_0, R is 0.65 (experiment) and 0.6 (model) and, at 2/3 V_0, is 0.34 (experiment) and 0.3 (model). In agreement with earlier work (Julian and Sollins, 1975; Ford et al., 1985), these results indicate that the reduction in force during sliding in the shortening direction is due to decrease in both the number of attached cross-bridges and the cross-bridge force. A reduced strain in the population of attached cross-bridges affects their distribution in favor of the state further ahead in the force-generating process. In fact, the fraction of attached cross-bridges in A3 state (A3/(A1 + A2 + A3)) is 0.3 at 1/3 V_0 and 0.4 at 2/3 V_0.

In Fig. 5 *B* the power velocity relations ($\dot{W}$-V) for the experiment (*solid line*) and for the model (*dashed line*) are calculated from the T-V relation in Fig. 5 *A*. For each of the two curves, both the power and the velocity are normalized for their respective V_0. The maximum value ($\dot{W}_{max}$, 0.12 $(T \cdot V)/(T_0 \cdot V_0)$, experiment; 0.11 $T \cdot V/T_0 \cdot V_0$, model) is attained at about 1/3 V_0 in both cases.

In summary, the simulated relations in Fig. 5 agree with the experimental ones in many respects. 1) The T-V relation deviates from the hyperbola in the region of high forces. This prediction of the model depends on the assumption of a very low probability for attachment at the edges of the range of positions accessible in isometric conditions. Thus, sliding brings detached cross-bridges to the region of higher attachment probability, and this per se partially counteracts the velocity-dependent decrease in force. 2) According to Huxley's 1957 model, V_0 is predicted by optimizing the x-dependence of the rate constant k_4 in the range $x < -9$ nm, where A3 cross-bridges become negatively strained. 3) The value of a/T_0 and, therefore, the maximum power output are somewhat lower in the simulation than in the experiment. The velocity of shortening for the maximum power output (1/3 V_0) is correctly predicted. The possibility of the model to predict these responses depends substantially on the contribution to force generation by cross-bridges detaching from A2 to D2 and rapidly reattaching. For further consideration on this point, see Discussion.

Fig. 6 *A* shows the steady-state fluxes of cross-bridges through the long stroke cycle (Φ_l) and through the short stroke cycle (Φ_s) in relation to sliding velocity. In isometric conditions, although Φ_l is practically zero, Φ_s has a value of 7.1 s^{-1}, because of the detachment of isometric cross-bridges from A2. This gives the model the property to predict the isometric heat production. Φ_l increases monotonically with the shortening velocity and attains the maximum value at V_0. For sliding velocities lower than 1/5 V_0,Φ_s increases with velocity much more steeply than Φ_l, contributing to the marked increase in rate of energy liberation ($\dot{E}$), as shown in Fig. 6 *B* (*circles*). At higher shortening speed, Φ_s decreases with velocity and the high level of $\dot{E}$ is maintained by the high level of Φ_l. $\dot{E}$ has its maximum (6.5 times the isometric plateau value) at 1/3–1/2 V_0 and then for larger velocities slightly reduces. To give the curve of the power output calculated from Fig. 5 *A*, the same dimensions as $\dot{E}$, the force relative to the isometric force (T/T_0) must be multiplied for the isometric force per myosin head (F_0, 1.93 pN). The corresponding power-velocity relation is shown by the filled

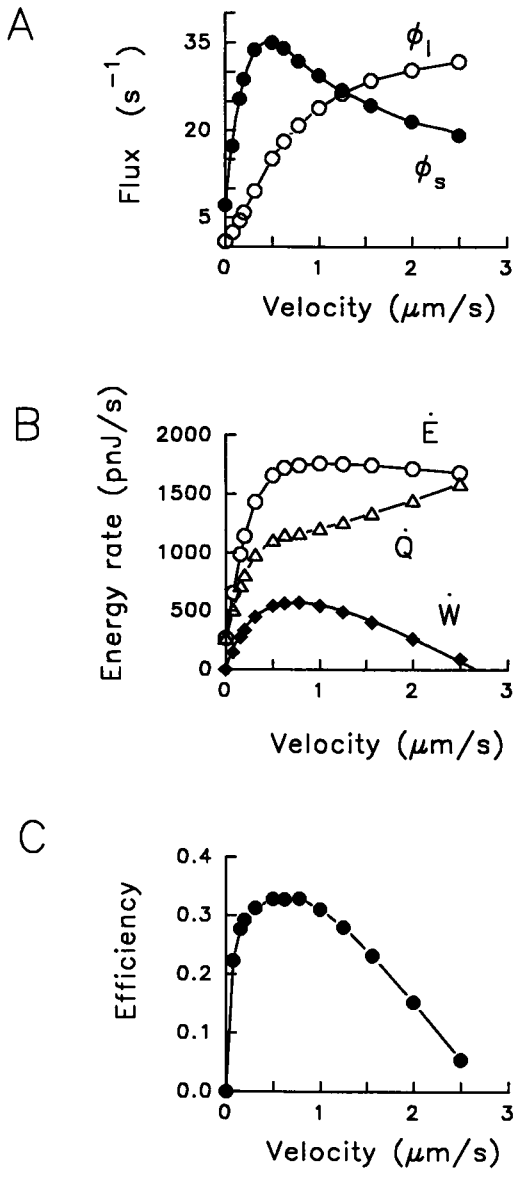

FIGURE 6 (*A*) Fluxes of cross-bridges through the short stroke cycle (●, Φ_s) and through the long stroke cycle (○, Φ_l) in relation to shortening velocity. (*B*) Relations of power (♦, $\dot{W}$), rate of energy liberation (○, $\dot{E}$) and rate of heat production (△, $\dot{Q}$) versus shortening velocity. (*C*) Relation of efficiency ($\dot{W}/\dot{E}$) versus shortening velocity. In the panels, with the exception of the power-velocity relation, the solid lines are drawn by eye through the data points.

diamonds in Fig. 6 *B*. The efficiency in energy conversion, calculated by the ratio of the power over the rate of energy liberation, is shown in Fig. 6 *C*. Efficiency attains the highest value (~0.33) at low shortening velocity (~1/5 V_0). Both maximum value and velocity dependence of efficiency are in satisfactory agreement with energetic data in the literature (Hill, 1939, 1964b; Woledge et al., 1985).

The expected rate of heat production ($\dot{Q}$) at any velocity of shortening can be calculated by subtracting $\dot{W}$ from $\dot{E}$ (*triangles* in Fig. 6 *B*). In isometric conditions, $\dot{W}$ is zero and $\dot{E}$ (266 pnJ/s) gives an estimate of maintenance heat (Hill, 1938, 1964a). For velocities lower than ~1/6 V_0, the slope of the relation $\dot{Q}$-V is substantially higher than for the upper range of velocities. The slope, normalized for F_0, the force per myosin head, can be compared with Hill's parameter α/T_0 (1964a): the value estimated in the range of high velocities (0.14) is comparable with the value in Hill's work, whereas that estimated for low velocities (0.94) is significantly higher.

Staircase shortening

In staircase shortening, a series of identical step releases are delivered to the tetanized fiber at regular time intervals (Fig. 7 *A*, *left*). The time interval between steps in the staircase can be adjusted so that the same average shortening velocity (estimated by the ratio of the step amplitude over the time interval) can be set for different step amplitudes. Independent of the step size, the tension transient elicited by each step attains steady-state characteristics when the overall shortening exceeds 12–15 nm, the same amount of shortening necessary to attain the constant force during steady shortening (Fig. 7 *B*, *left*).

At the steady-state during staircase shortening, for a given shortening velocity the tension attained before the step, T_i/T_0, is almost the same independent of the step size.

The response of the model to ramp and staircase shortening is shown in the right panels of Fig. 7.

DISCUSSION

Mechanical and energetic properties of the model

The mechanical-kinetic model described in this paper combines the properties of Huxley's 1957 model, which explains most of the steady-state mechanical and energetic features of shortening muscle, and the properties of Huxley and Simmons' 1971 model, which interprets the tension transient after a step perturbation in length in terms of the working stroke of the attached cross-bridge. More specific properties of the contracting muscle such as the rate of regeneration of the working stroke, the way steady-state force is attained in response to ramp and staircase shortening, the isometric maintenance heat rate, the dependence of energy rate on shortening velocity are also satisfactorily described for the first time by the cross-bridge model in this paper. Even though a precise correspondence between the mechanical cycle described here and the biochemical cycle of the cross-bridges is not given, the model is energetically correct because for any given mechanical condition, the rate of energy liberation $\dot{E}$ assumes values in accordance with data in the literature.

Our simulated energy rates are in satisfactory agreement with data reported in the literature for frog muscle at 0°C. In fact, at 0°C the isometric maintenance heat rate is 14 mJ g^{-1} s^{-1} (Hill and Woledge, 1962; Woledge et al., 1985), which, with a concentration of myosin heads in muscle of 0.24 μM g^{-1}, correspond to 100 pnJ s^{-1} per myosin head. Taking into account that the simulation refers to experiments made on

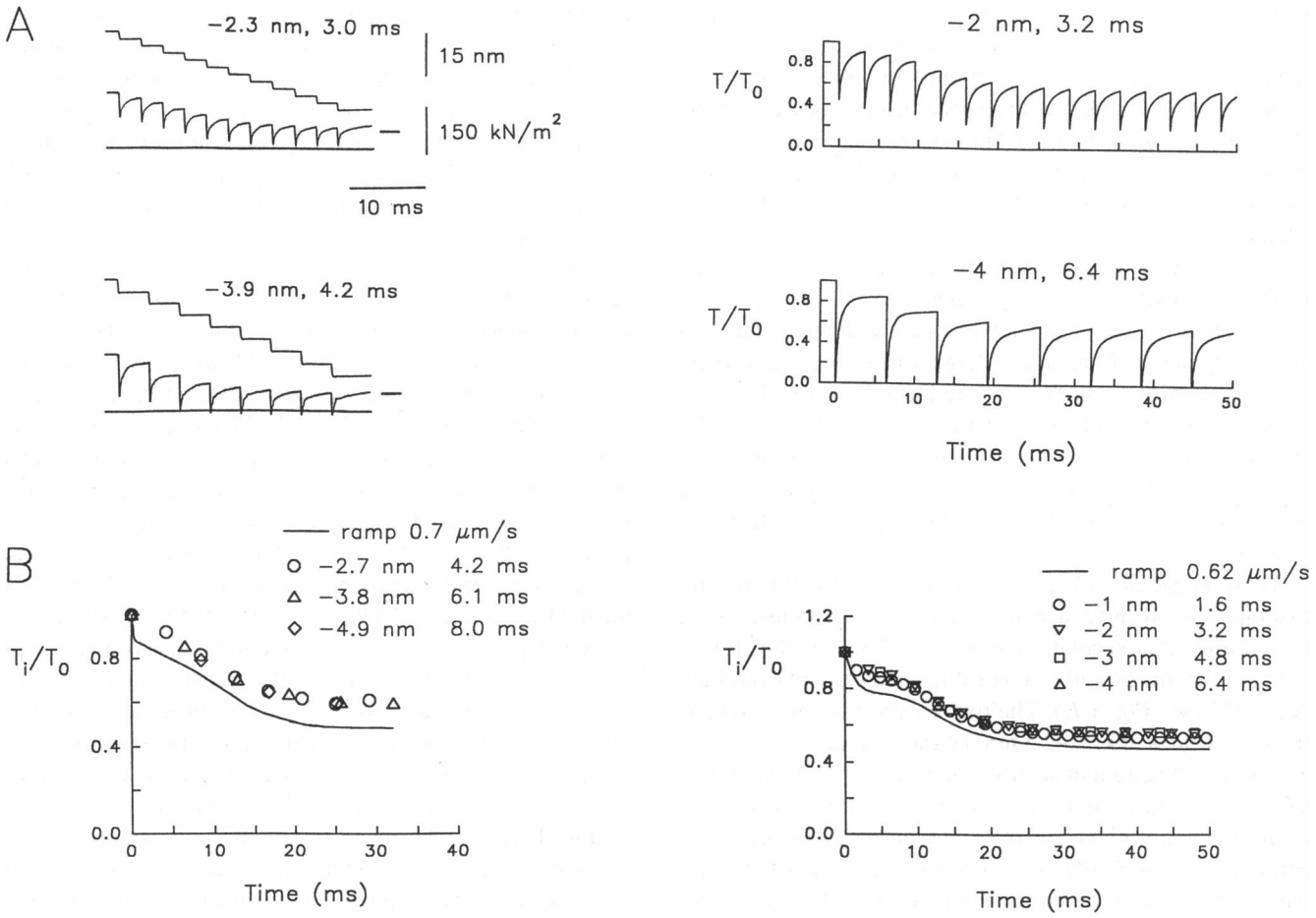

FIGURE 7 Tension responses to staircase shortening. (*left*) Experiment; (*right*) simulation. (*A*) In the experiment panel: (*top*) sarcomere length change; (*middle*) tension response; (*bottom*) resting tension; the horizontal bar on the right of the tension traces indicates the level of steady tension during ramp shortening at a velocity similar to the average velocity of staircase shortening. In both experiment and model panels, the sizes of step and pause are indicated above each record. (*B*) Relation between T_i/T_0 (the tension before each step in the staircase, made relative to the isometric tetanic tension) and time elapsed after the first step, for staircase shortening made by combining step sizes and pauses (as listed in the *inset*), so that the average velocity in each staircase is similar (~0.62 μm/s). The solid line is the tension during ramp shortening at the velocity indicated in the inset.

frog fibers at 4–5°C and that the Q_{10} for rate of heat production is >5 (Woledge et al., 1985), our value of 270 pnJ s^{-1} at 4–5°C is comparable with the value reported in the literature.

The maximum values of $\dot{E}$, attained at 1/3–1/2 V_0, is 6.5 times higher than the isometric value; thus, the increase is slightly larger than that reported in the literature (~4, Kushmerick and Davies, 1969; Woledge et al., 1985). Beyond 1/2 V_0, in agreement with experimental results, $\dot{E}$ decreases by a small amount.

The observed dependence of efficiency on shortening velocity (Hill, 1939, 1964b) is correctly predicted by the model. However, the maximum value (0.33) is somewhat lower than that reported in the literature for fast muscle of the frog (~0.4). The efficiency in the model could be increased by reducing the energy difference between the minima of the free energy curves of the attached states and the neighboring detached states. In particular, the energy drop between D2 free energy level and the minimum of A1 free energy curve, 17 pnJ (2.5 times the energy drop between D1 free energy level and minimum of A1 curve, Fig. 1 *A*) could be reduced, still maintaining a smaller efficiency for the cycle with 5-nm working distance. However, in this case, the drop in free energy implied in the short stroke cycle would be lower than that implied in the long stroke cycle and the free energy level of a cross-bridge in either state A1 or A2 for a given value of x would depend on the pathway through which the state is populated. Consequently, the number of states to be defined according to their free energy curves would increase. To maintain the reaction scheme at the maximum degree of simplicity permitted to fit the mechanical properties, we accepted the actual limit in the simulation of efficiency.

Necessity of two kinetically distinct pathways in cross-bridge interaction

The model shows that, depending on the mechanical conditions under which contraction occurs, cycles of cross-bridge attachment, force generation, and detachment follow two different pathways, distinct for the kinetics and for the

proportion of free energy converted into work. In the long stroke cycle, the cross-bridge detaches at the end of the working stroke (sliding distance ~ 10 nm) and reattaches further along the actin filament with a speed that is moderate. In the short stroke cycle, detachment occurs at an intermediate stage during the working stroke (sliding distance ~ 5 nm) and is followed by rapid reattachment further along the actin filament.

Shortening at low speed increases the probability of the short stroke cycle; A2 cross-bridges detach at x values >−5 nm (i.e., before exerting negative forces) and rapidly reattach at the original position and undergo a new force-generating step. Shortening at high speed reduces the probability of short stroke cycle and increases that of the long stroke cycle; A3 cross-bridges detach for x values <−9 nm, where they exert negative forces and, because reattachment occurs at a moderate rate, the number of attached cross-bridges decreases.

These properties of the model are provided by specific assumptions on the x-dependence of the rate constants k_3, controlling the second step (A2 → A3) in the force-generating process, and k_5, controlling detachment from state A2 to D2 (see Fig. 1 *E*). The two k values become comparable for values of $x \sim -2.5$ nm, i.e., where A2 cross-bridges are still exerting a small positive force. The underlying physical event could be that the myosin head, for a given configuration and a given relative position with respect to the actin site to which it is attached, once executed the 5-nm working stroke, undergoes a relatively rapid (~100/s) process of detachment and reattachment to the nearest actin site in an attitude that allows a new complete working stroke. Either Φ_s or Φ_l has the maximum at the shortening velocity for which their respective detachment step attains the maximum speed. For the short stroke cycle, this condition occurs at ~0.6 μm/s (~1/5 V_0): at this velocity there is enough time for A2 cross-bridges to undergo the ~100/s detachment process while traveling from 0 to −5 nm. This is a condition for maximum power output because most of cross-bridges, whichever is the state, are exerting positive forces. For the long stroke cycle, the maximum flux through the detachment step occurs at the maximum velocity of shortening. The increase in Φ_l is accompanied by the increase of the fraction of A3 cross-bridges exerting negative forces and by the reduction of the power output.

The constraints under which the process of early detachment followed by rapid reattachment occurs are made evident by the double-step experiment simulation. A conditioning step release of 5 nm is able to elicit the rapid regeneration process for most of the cross-bridges, whereas a larger step is not. At the same time, if the test step is delivered too early, before the regeneration process is complete, it will produce the same effects as a larger step given alone. It is evident from this behavior that the possibility to elicit the fast detachment-reattachment process, implying 5-nm working stroke (steps 5 and 6), or the slow detachment-reattachment process, implying 10-nm working stroke (steps 4 and 1), depends on both the relative position between the myosin head and the actin site and the time elapsed in that position with respect to the time constant of the regeneration process. These two factors determine the ability of the model to simulate satisfactorily the rapid regeneration of the working stroke as well as the relations of force, power, energy rate, and efficiency versus velocity of steady shortening.

Note that if the isometric force per cross-bridge is 3 times larger than that assumed here, 7.5 pN instead of 2.5 pN, the correct efficiency in energy conversion is attained with only one cross-bridge interaction per ATP hydrolyzed, through either the l or the s pathway. Also, in this case if we retain the constraint of the two kinetically distinct pathways for the cross-bridge interaction, the model predicts both the correct power output and the decrease of the rate of energy liberation for shortening velocities >1/2 V_0. With a one-to-one coupling, in either the short or the long stroke cycle the free energy consumption corresponds to the energy liberated by the hydrolysis of one ATP molecule, but in the first case the detached state is ready to reattach quickly (according to our k_6), whereas in the latter case reattachment occurs at a moderate rate (according to our k_1). In biochemical terms, this idea means that the mechanical conditions that favor detachment to D1 imply that the unattached cross-bridge must undergo a time consuming transition between different biochemical states to be ready for another interaction.

If the force per cross-bridge is 7.5 pN, the fraction of heads involved in isometric force development is 3 times smaller than that assumed here and stiffness in the half-sarcomere is not a reliable estimate of the fraction of attached heads, as suggested by recent structural data (Huxley et al., 1994; Wakabayashi et al., 1994).

A common drawback of cross-bridge models, in which ATP hydrolysis occurs only with the completion of the working stroke (Huxley, 1957, 1980; Julian et al., 1974; Eisenberg et al., 1980; Pate and Cooke, 1989), is that the rate of energy liberation continues to increase with the increase in shortening velocity, even for velocities >1/2 V_0. Actually, to explain the observed decline of the rate of energy liberation at high velocities, A. F. Huxley (1973) modified his 1957 model by assuming that attachment takes place in two steps, so that cross-bridges can attach and detach without implying ATP hydrolysis. In his case, however, cross-bridges detach at the beginning of the cycle without entering the working part of the cycle. Therefore, his hypothesis is not adequate to explain the rapid working stroke regeneration by cross-bridges already exerting the isometric force. In a recent paper (Cooke et al., 1994), the expected relation of energy rate versus velocity of steady shortening has been obtained by assuming that, with the increase in shortening velocity, a progressively larger fraction of cross-bridges interacts without commitment for ATP splitting, because it detaches in the negative range of x, once it attains a sufficiently high free energy level at the expense of the fraction of cross-bridges interacting in the positive range of

x. The limit of this assumption is that it implies a very low power output at intermediate and high velocities. Indeed, as originally emphasized by A. F. Huxley (1957), detachment in the negative range of x must be rather quick if we want to preserve the power and the efficiency of shortening muscle.

Maintenance heat

An important energetic aspect that can be accommodated under the assumptions made in this model is the relatively high rate of maintenance heat (Hill, 1938). In a model (e.g., Huxley and Simmons, 1971) in which the force generation is based on a few state transitions controlled by strain-dependent rate constants, the probability for an attached head to go through the whole working stroke in isometric conditions is necessarily low. In fact, to ensure a 4-nm pre-step extension in the instantaneous elasticity (as measured by the abscissa intercept of T_1 curve) and a 11–12 nm sliding distance for which attached cross-bridges can exert force (as measured by the abscissa intercept of T_2 curve), the pre-step distribution must be biased to the beginning of the working stroke. Consequently, conventional models with a possibility of detachment only at the end of the working stroke suffer an intrinsic difficulty to explain the relatively high rate of maintenance heat. The presence in our model of an isometric flux of energy accompanying detachment from an intermediate stage in the force-generating process provides a straightforward explanation for the maintenance heat production. The correlation existing in different fiber types between the rate of isometric heat production and the maximum power (Woledge et al., 1985; Barclay et al., 1994) supports the idea in this model that power output in shortening muscle is increased by increasing the rate constant controlling early detachment (A2 → D2) at the expense of efficiency in energy conversion.

The assumption that the cross-bridge cycle with early detachment followed by fast reattachment implies a lower fraction of free energy to be converted into work provides a clue for explaining why in different muscles the higher the power output, the lower the efficiency (Woledge, 1968). By reducing the rate constant controlling early detachment (A2 → D2), cross-bridges cycle with an intrinsically lower speed, mainly through the long stroke cycle, so that the overall efficiency in energy conversion is higher at the expense of maximum power output.

Fraction of heads attached in isometric conditions and number of interactions per ATP hydrolyzed

The assumption in the model that the force developed by a cross-bridge in isometric conditions is 2.5 pN implies a substantially high fraction of myosin heads (77%) attached in isometric conditions. This is supported by the following structural and mechanical evidence. 1) Time-resolved x-ray diffraction studies show that the signals related to the mass distribution of myosin heads are strongly affected either during isometric force development (Huxley and Brown, 1967; Matsubara et al., 1975; H. E. Huxley et al., 1980) or during the synchronous execution of the elementary force-generating step (Irving et al., 1992). 2) Stiffness in an isometric contraction is a large fraction of rigor stiffness (Goldman and Simmons, 1977). 3) During sliding at low speed in the lengthening direction, a condition under which detachment is slow, the increase in number of attachments is compatible with 20–30% residual cross-bridges not attached in isometric conditions (Lombardi and Piazzesi, 1990).

According to Huxley and Simmons theory of force generation, the force per attached cross-bridge must be sufficiently low (~2.5 pN) to be able to predict correctly the kinetics of the quick force recovery after a step under the assumption that the mechanical energy involved in the two force-generating transitions is part of the activation energy for the transitions (Piazzesi et al. 1992). In turn, with an isometric force of 2.5 pN, the maximum energy delivered in a single working stroke, about 20 pnJ from Huxley and Simmons' T_2 curve (1971), is too low to account for the relatively high efficiency of energy conversion (Hill, 1939, 1964a). The contradiction is solved if there is more than one working stroke per molecule of ATP hydrolyzed, as first hypothesized by Yanagida et al. (1985). Measurements in a new in vitro assay (Finer et al., 1994), showing that under low load the sliding distance per cross-bridge interaction is 11 nm and that under near isometric conditions the average force per interacting cross-bridge is 3.4 pN, seem to confirm that the mechanical energy implied in one working stroke is too low to account for the high muscle efficiency. However, the same authors believe that their force and displacement values are underestimated.

As to the mechanism underlying the one-to-many relation between ATP hydrolysis and mechanically identified cross-bridge interactions, it seems unlikely the presence of a soluble compound responsible for the fractionation of the free energy of ATP hydrolysis. In fact, the recent acquisitions on the crystal structure of S1 portion of the myosin molecule (Rayment et al., 1993) confirm the tight relation between the site where hydrolysis occurs and products are released and the site responsible for the conformational change inducing the working stroke. An alternative hypothesis is that the mechanism responsible for multiple work producing interactions is in the myosin molecule itself. In this relation, a detailed structural model should incorporate the explanation for the finding that, during the 1000/s conformational change accompanying the working stroke, the myosin head moves so as to spread the density distribution of the mass projections on the filament axis, and successively reattains the original configuration at a rate of 100/s (Irving et al., 1992).

Alternative hypotheses for the rapid regeneration of the working stroke

Recently, some hypotheses have been made to explain the rapid regeneration of the 12-nm working stroke, without con-

tradiction with the concept of tight coupling between the ATPase cycle and the mechanical cycle. One hypothesis (A. F. Huxley, 1993) assumes that the two heads of the myosin molecule work in sequence, the second head being energized by the stroke of the first, with only one molecule of ATP split. An alternative hypothesis (A. F. Huxley, 1992) is that the release of P_i, promoted by the partial working stroke underlying the quick recovery elicited by the conditioning release, resets the actin-myosin complex to the beginning of the working stroke. We tried to simulate mechanical results with a model that implies only the long stroke cycle and only one process of rapid regeneration of the working stroke. Under these assumptions, we could simulate the responses to double-step releases, but we failed to predict correctly several mechanical properties: 1) the curvature of the *T-V* relation is too large and the maximum power output is too low; 2) during ramp or staircase shortening, steady-state characteristics are attained through a transitory depression of the force response below that at the steady state, which are not present in the experimental records.

Other hypotheses that account for the rapid regeneration of the working stroke without postulating rapid cross-bridge detachment and reattachment (Huxley and Kress, 1985; Chen and Brenner, 1993) imply that a small fraction of cross-bridges is responsible for force generation at any time during contraction. Regeneration of the working stroke in this case involves not fast cycling but fast state transitions with replacement of cross-bridges, which have already gone through the working stroke, with a new cross-bridge population. Even under the hypothesis of only 25% of myosin heads attached, Chen and Brenner's (1993) simulation of staircase shortening fails to fit the experimental records as regards the transition to the steady state: there is a depression in the tension response in correspondence of the third step (their Fig. 4). However, with a kinetic scheme similar to that in our model, if the rapid regeneration of the working stroke can occur 3 times (Piazzesi et al., 1994), it is possible to fit the transition to the steady-state force response to staircase shortening. Note that the above assumption is equivalent to the hypothesis that the fraction of cross-bridges attached in isometric conditions is ~1/4 of the total heads, so that the original isometric population can be rapidly replaced 3 times. In any case, both Chen and Brenner (1993) and Piazzesi et al. (1994) simulations suffer of the limit common to all cross-bridge models in which ATP hydrolysis occurs only with the completion of the working stroke: the rate of energy liberation continues to increase with the increase of shortening velocity beyond 1/2 V_0.

Step size per cross-bridge interaction

The sliding distance accounted for by each of the two steps in the force-generating transition is 4.5 nm. Because the range of positions for attachment extends from 3.9 to −1.6 nm and the average isometric extension is ~1 nm, the total working distance per interaction is ~5.5 nm for the short stroke cycle and ~10 nm for the long stroke cycle. The two types of cross-bridge cycles assumed in the model are identified only for their kinetic, mechanical, and energetic properties but provide useful implications for the underlying structural changes. In fact, it has been shown (Irving et al., 1992) that a very simple structural model, which combines the assumption in our model of either ~5- or ~10-nm working distance per cross-bridge interaction (Piazzesi et al., 1992) with the original H. E. Huxley (1969) hypothesis of swinging heads, can simulate satisfactorily both the amount and the time course of myosin head movements associated with the working stroke and its regeneration. In addition, it must be noted that our assumption of a load-dependent probability of cross-bridges to perform a working stroke of either 5 nm (high load) or 10 (low load) nm agrees with the estimates in in vitro assays (Finer et al., 1994; Ishijima et al., 1994).

In our model, because the proportion of myosin cross-bridges undergoing either one or two 5-nm steps per interaction changes with the speed of steady shortening, the average working distance per interaction will change accordingly, going from 6.5 nm at 1/5 V_0 to 8.1 nm at V_0.

We are grateful to Dr. Malcolm Irving for criticism and suggestions on a preliminary version of the paper. We thank our co-worker Dr. Marco Linari for letting us include unpublished records and graphs from a recent series of experiments on staircase shortening. We also thank Ms. Chiara Balestri for the help given in the calculation process and Mr. Adrio Vannucchi for the preparation of illustrations.

This work was supported by grants from the Italian M.U.R.S.T., the Italian C.N.R. and Telethon (Italy, grant 239).

REFERENCES

Bagshaw, C. R. 1993. Muscle Contraction. Chapman & Hall, London. 155 pp.

Barclay, C. J., J. K. Constable, and C. L. Gibbs. 1993. Energetics of fast- and slow-twitch muscles of the mouse. *J. Physiol.* 472:61–80.

Cecchi, G., F. Colomo, and V. Lombardi. 1976. A loudspeaker servo system for determination of mechanical characteristics of isolated muscle fibres. *Boll. Soc. Ital. Biol. Sper.* 52:733–736.

Cecchi, G., F. Colomo, and V. Lombardi. 1978. Force-velocity relation in normal and nitrate-treated frog single muscle fibres during rise of tension in an isometric tetanus. *J. Physiol.* 285:257–273.

Chen, Y., and B. Brenner. 1993. On the regeneration of the actin-myosin power stroke in contracting muscle. *Proc. Natl. Acad. Sci. USA.* 90:5148–5152.

Cooke, R., H. White, and E. Pate. 1994. A model of the release of myosin heads from actin in rapidly contracting muscle fibers. *Biophys. J.* 66: 778–788.

Edman, K. A. P., L. A. Mulieri, and B. Scubon-Mulieri. 1976. Non-hyperbolic force-velocity relationship in single muscle fibres. *Acta Physiol. Scand.* 98:143–156.

Eisenberg, E., T. L. Hill, and Y. Chen. 1980. Cross-bridge model of muscle contraction. *Quant. Anal. Biophys. J.* 29:195–227.

Fenn, W. O. 1924. The relation between work performed and the energy liberated in muscular contraction. *J. Physiol.* 58:373–395.

Finer, J. T., R. M. Simmons, and J. A. Spudich. 1994. Single myosin molecule mechanics: piconewton forces and nanometre steps. *Nature.* 368: 113–119.

Ford, L. E., A. F. Huxley, and R. M. Simmons. 1977. Tension responses to sudden length change in stimulated frog muscle fibres near slack length. *J. Physiol.* 269:441–515.

Ford, L. E., A. F. Huxley, and R. M. Simmons. 1981. The relation between stiffness and filament overlap in stimulated frog muscle fibres. *J. Physiol.* 311:219–249.

Ford, L. E., A. F. Huxley, and R. M. Simmons. 1985. Tension transients during steady shortening of frog muscle fibres. *J. Physiol.* 361:131–150.

Goldman, Y. E., and R. M. Simmons. 1977. Active and rigor muscle stiffness. *J. Physiol.* 269:55P–57P.

Gordon, A. M., A. F. Huxley, and F. J. Julian. 1966. The variation in isometric tension with sarcomere length in vertebrate muscle fibres. *J. Physiol.* 184:170–192.

Hill, A. V. 1938. The heat of shortening and the dynamic constants of muscle. *Proc. R. Soc. Lond. Ser. B.* 126:136–195.

Hill, A. V. 1939. The mechanical efficiency of frogs' muscle. *Proc. R. Soc. Lond. Ser. B.* 127:434–451.

Hill, A. V. 1964a. The effect of load on the heat of shortening of muscle. *Proc. R. Soc. Lond. Ser. B.* 159:297–318.

Hill, A. V. 1964b. The efficiency of mechanical power development during muscular shortening and its relation to load. *Proc. R. Soc. Lond. Ser. B.* 159:319–324.

Hill, A. V., and R. C. Woledge. 1962. An examination of absolute values in myothermic measurement. *J. Physiol.* 162:311–333.

Hill, T. L. 1974. Theoretical formalization for the sliding filament model of contraction of striated muscle. Part I. *Prog. Biophys. Mol. Biol.* 28:267–340.

Homsher, E., M. Irving, and A. Wallner. 1981. High-energy phosphate metabolism and energy liberation associated with rapid shortening in frog skeletal muscle. *J. Physiol.* 321:423–436.

Huxley, A. F. 1957. Muscle structure and theories of contraction. *Prog. Biophys. Biophys. Chem.* 7:255–318.

Huxley, A. F. 1973. A note suggesting that cross-bridge attachment during muscle contraction may take place in two stages. *Proc. R. Soc. Lond. Ser. B.* 183:83–86.

Huxley, A. F. 1974. Muscular contraction. *J. Physiol.* 243:1–43.

Huxley, A. F. 1980. Reflections on Muscle. Liverpool University Press. 107 pp.

Huxley, A. F. 1992. A fine time for contractual alterations. *Nature.* 357: 110*a*. (Abstr.)

Huxley, A. F., 1993. Mechanism of Myofilament Sliding in Muscle Contraction. H. Sugi and G. H. Pollack, editors. Plenum Publishing Corporation, New York. 839–847.

Huxley, A. F., and V. Lombardi. 1980. A sensitive force transducer with resonant frequency 50 kHz. *J. Physiol.* 305:15P–16P.

Huxley, A. F., and R. M. Simmons. 1971. Proposed mechanism of force generation in striated muscle. *Nature.* 233:533–538.

Huxley, A. F., and R. M. Simmons. 1973. Mechanical transients and the origin of muscular force. *Cold Spring Harbor Symp. Quant. Biol.* 37: 669–680.

Huxley, A. F., V. Lombardi, and L. D. Peachey. 1981. A system for fast recording of longitudinal displacement of a striated muscle fibre. *J. Physiol.* 317:12P–13P.

Huxley, H. E. 1969. The mechanism of muscular contraction. *Science.* 164: 1356–1366.

Huxley, H. E., and W. Brown. 1967. The low-angle x-ray diagram of vertebrate striated muscle and its behavior during contraction and rigor. *J. Mol. Biol.* 30:383–434.

Huxley, H. E., A. R. Faruqi, J. Bordas, M. H. J. Koch, and J. R. Milch. 1980. The use of synchrotron radiation in time-resolved x-ray diffraction studies of myosin layer-line reflections during muscle contraction. *Nature.* 284: 140–143.

Huxley, H. E., and M. Kress. 1985. Crossbridge behaviour during muscle contraction. *J. Muscle Res. Cell Motil.* 6:153–161.

Huxley, H. E., A. Stewart, H. Sosa, and T. Irving. 1994. X-ray diffraction measurements of the extensibility of actin and myosin filaments in contracting muscle. *Biophys. J.* 67:2411–2421.

Infante, A. A., D. Klaupiks, and R. B. Davies. 1964. Adenosine triphosphate: changes in muscles doing negative work. *Science.* 144:1577–1578.

Irving, M., V. Lombardi, G. Piazzesi, and M. A. Ferenczi. 1992. Myosin head movements are synchronous with the elementary force-generating process in muscle. *Nature.* 357:156–158.

Ishijima, A., Y. Harada, H. Kojima, T. Funatsu, H. Higuchi, and T. Yanagida. 1994. Single-molecule analysis of the actomyosin motor using nano-manipulation. *Biochem. Biophys. Res. Commun.* 199: 1057–1063.

Julian, F. J., K. R. Sollins, and M. R. Sollins. 1974. A model for the transient and steady-state mechanical behavior of contracting muscle. *Biophys. J.* 14:546–562.

Julian, F. J., and M. R. Sollins. 1975. Variation of muscle stiffness with force at increasing speeds of shortening. *J. Gen. Physiol.* 66:287–302.

Katz, B. 1939. The relation between force and speed in muscular contraction. *J. Physiol.* 96:45–64.

Kushmerick, M. J., and R. E. Davies. 1969. The chemical energetics of muscle contraction. II. The chemistry, efficiency and power of maximally working sartorius muscles. *Proc. R. Soc. Lond. Ser. B.* 174:315–353.

Lännergren, J. 1978. The force-velocity relation of isolated twitch and slow muscle fibres of Xenopus laevis. *J. Physiol.* 283:501–521.

Lombardi, V., and G. Piazzesi. 1990. The contractile response during steady lengthening of stimulated frog muscle fibres. *J. Physiol.* 431:141–171.

Lombardi, V., G. Piazzesi, and M. Linari. 1992. Rapid regeneration of the actin-myosin power stroke in contracting muscle. *Nature.* 355:638–641.

Lymn, R. W., and E. W. Taylor. 1971. Mechanism of adenosine triphosphate hydrolysis by actomyosin. *Biochemistry.* 10:4617–4624.

Matsubara, I., N. Yagi, and H. Hashizume. 1975. Use of an x-ray television for diffraction of the frog striated muscle. *Nature.* 255:728–729.

Pate, E., and R. Cooke. 1989. A model of crossbridge action: the effects of ATP, ADP and Pi. *J. Muscle Res. Cell Motil.* 10:181–196.

Piazzesi, G., F. Francini, M. Linari, and V. Lombardi. 1992. Tension transients during steady lengthening of tetanized muscle fibres of the frog. *J. Physiol.* 445:659–711.

Piazzesi, G., M. Linari, and V. Lombardi. 1993. Mechanism of Myofilament Sliding in Muscle Contraction. H. Sugi and G. H. Pollack, editors. Plenum Publishing Corporation, New York. 691–700.

Piazzesi, G., M. Linari, and V. Lombardi. 1994. Kinetic requirements to simulate steady state and transient characteristics of contracting muscle. *Pflügers Arch.* 426:R178/55.

Rayment, I., H. M. Holden, M. Whittaker, C. B. Yohn, M. Lorenz, K. C. Holmes, and R. A. Milligan. 1993. Structure of the actin-myosin complex and its implications for muscle contraction. *Science.* 261:58–65.

Wakabayashi, K., Y. Sugimoto, H. Tanaka, Y. Ueno, Y. Takezawa, and Y. Amemiya. 1994. X-ray diffraction evidence for the extensibility of actin and myosin filaments during muscle contraction. *Biophys. J.* 67:2422–2435.

Woledge, R. C. 1968. The energetics of tortoise muscle. *J. Physiol.* 197: 685–707.

Woledge, R. C., N. A. Curtin, and E. Homsher. 1985. Energetic Aspects of Muscle Contraction. Academic Press, London. 329 pp.

Yanagida, T., T. Arata, and F. Oosawa. 1985. Sliding distance of actin filament induced by a myosin cross-bridge during. *Nature.* 316:366–369.